JOURNAL OF VOLCANOLOGY AND SEISMOLOGY, 2025, No. 1, pp. 3–16

# EXPLOSIVE ACTIVITY OF ZAVARITSKY VOLCANO (SIMUSHIR ISLAND, CENTRAL KURILES) DURING THE HOLOCENE

© 2025 O. V. Dirksen[a, *], V. V. Ponomareva[a], E. A. Zelenin[b], P. Yu. Plechov[c], T. M. Philosofova[a] and A. V. Rybin[d]

[a]*Institute of Volcanology and Seismology FEB RAS, Petropavlovsk-Kamchatsky, Russia*
[b]*Geological Institute RAS, Moscow, Russia*
[c]*Fersman Mineralogical Museum RAS, Moscow, Russia*
[d]*Institute of Marine Geology and Geophysics FEB RAS, Yuzhno-Sakhalinsk, Russia*
**e-mail: oleg.dirksen@gmail.com*

Received July 05, 2024
Revised September 01, 2024
Accepted October 20, 2024

**Abstract.** In our paper we represent the first data on the Holocene explosive activity of Zavaritsky volcano, the largest caldera center on Simushir Island (Central Kuriles). For the first time, we reconstructed the chronology of explosive eruptions of this volcanic center for the past 10 000 years, as well as estimate the parameters of its largest eruptions. In total, more than 40 tephra horizons have been identified, which allows us to estimate the frequency of eruptions: 1 event in 250 years. Constructed age model allowed us to determine the age of most eruptions. Volcanic glasses of Holocene tephras correspond in composition to low-potassium basaltic andesite-rhyolites, while the very low $K_2O$ content makes it possible to fairly confidently distinguish Zavaritsky tephra not only from the tephra of neighboring moderate-potassium volcanoes, but also from the tephra of other low-potassium volcanoes of the Kuril-Kamchatka Island arc.

Holocene activity of Zavaritsky volcano started with two powerful eruptions with a conservatively estimated magnitude (M) of 6.4 and 5.6, which occurred about 9.5 and 9.2 thousand years ago (ka BP). Tephra from the first eruption (ZV-1) spread to the northeast and was found as far as northwestern North America. Tephra from the second powerful eruption (ZV-3) spread north and was found in sediments of the Sea of Okhotsk. Volcanic glass of ZV-1 tephra is characterized by rhyolitic composition with the highest $SiO_2$ content (72.5–74 wt. %). Glasses of the ZV-3 tephra varied in composition from dacites to rhyodacites (65–71.9 wt. % $SiO_2$). The products of subsequent eruptions were represented by cinder with glasses of dacite — andesite and basaltic andesite composition. Dacitic glasses reappeared only in the tephra of the last large explosive eruption that occurred early before the middle of the 19th century.

Our studies revealed the catastrophic explosive eruptions of Zavaritsky volcano during the Early Holocene and sustained activity of this eruptive center throughout the Holocene. The appearance of high-silica glasses in the tephra of the last powerful eruption (ZV-40) indicates a possible strong eruption in the near future.

**Keywords:** *Zavaritsky volcano, caldera, explosive eruption, tephra, Kurile Islands, volcanic glass composition, Holocene*

**DOI:** 10.31857/S02030306250101e4

## INTRODUCTION

One of the important natural processes affecting Earth's climate, which needs to be considered in forecast models, is large-scale explosive volcanism [Baldini et al., 2015; McConnell et al., 2020]. Numerous attempts to establish the causes of explosive activity outbursts and understand their connection with geodynamics and/or climate changes have not yet been successful, primarily due to the lack of accurate and detailed chronicles of eruptions over long periods of time. Reconstructing explosive activity within island arcs presents a particular challenge, as their pyroclastic deposits are often hidden underwater, and on land they form complex and partially eroded sequences. One such arc is the Kuril segment of the Kuril-Kamchatka volcanic belt in the northwestern Pacific Ocean. Evidence of repeated powerful eruptions here includes numerous calderas and layers of pumice deposits [Gorshkov, 1967], but the record of past eruptions has so far been deciphered only fragmentarily and for only a few volcanoes [Degterev et al., 2012; Hasegawa et al., 2011; Nakagawa et al., 2002]. In this article, we compare the results of studying terrestrial pyroclastics with published data on ashes buried in marine and terrestrial sediments to reconstruct for the first time the chronology of explosive eruptions of Zavaritsky volcano (Simushir Island, Kuril Islands) over the past 10,000 years and to estimate the parameters of its largest eruptions.

The Zavaritsky volcano is located in the central part of Simushir Island (Central Kuriles) (Fig. 1a). It represents a shield-like volcanic edifice with a diameter of about 17 km, cut by two nested calderas. The diameter of the outer, older caldera is about 10 km, while the inner, younger one is 7–8 km [Gorshkov, 1967]. Subsequent eruptions formed a stratovolcano with a base diameter of about 6 km inside the young caldera, the summit of which was also destroyed as a result of powerful explosive eruptions. The resulting crater (caldera?) measuring 3.5 × 2.7 km is currently filled with Lake Biryuzovoe, which contains two small extrusive domes. The volcanic massif is composed of rocks of the low-potassium calc-alkaline series [Parfenova et al., 2015].

The only recorded eruptions of this center occurred in 1916–1932 and in 1957, resulting in the formation of the Eastern and Northern domes, respectively [Gorshkov, 1967], however, tephra from these eruptions was not found outside the caldera. Information about older eruptions, including caldera-forming ones, and the age of the volcano as a whole is very scarce and contradictory. Analysis of the morphology of the slopes of both calderas suggested that they formed in the Middle-Late Pleistocene [Gorshkov, 1967] or at the very end of the Upper Pleistocene glaciation or immediately after it [Melekestsev et al., 1974]. Deposits of the Holocene soil-pyroclastic cover (hereinafter SPC) in the vicinity of the volcano, including numerous tephra horizons, were described in [Razzhigaeva et al., 2013], but these studies were primarily focused on the development of island landscapes rather than eruption history. Studies of distal Holocene ashes on other islands of the Kuril chain, as well as in cores from marine sedimentary columns, allowed two ash horizons to be associated with Zavaritsky volcano. The first is an early Holocene ash that spread as far as Shumshu Island, initially dated to ~8.9 thousand years (all age values in the article are given in calibrated years before 1950) [Nakagawa et al., 2008]. A low-potassium ash was also found in the sedimentary columns of the Sea of Okhotsk, initially described as tephra from the Tao-Rusyr caldera, but in subsequent works attributed to Zavaritsky volcano with the index TR(Zv) [Derkachev et al., 2016]. Cryptotephra from Zavaritsky volcano was found in a peat bog in northwestern Canada, where its age was estimated at 9560 ± 110 years [Davies et al., 2018]. At the same time, isolated descriptions of proximal pyroclastic sections on Simushir Island did not allow determining whether the discovered ashes were the result of a single catastrophic eruption or were formed as a result of a series of powerful eruptions. In addition, another tephra from Zavaritsky volcano (Zav-1) was found on the islands of Chirpoi and Urup [Nakagawa et al., 2008; Razjigaeva et al., 2022]. Its age was previously estimated in the range

of 1000–600 years ago (ya) [Nakagawa et al., 2008; Razjigaeva et al., 2022]. Other information about eruptive activity within the Zavaritsky volcanic center was absent.

## MATERIALS AND METHODS

During the fieldwork in 2011 on Simushir Island, we described more than 20 sections of Holocene soil-pyroclastic covers (SPC), in which at least 40 horizons of pyroclastic material from Zavaritsky volcano were identified, and more than 160 samples of its tephra were collected (Fig. 1a, 1b). The determination of major rock-forming oxides content in volcanic glasses was performed at the Faculty of Geology, Moscow State University, using energy-dispersive electron probe analysis (Oxford X-MaxN spectrometer with a crystal area of 80 $mm^2$, installed on a JEOL JSM-6480LV electron microscope). The analysis was conducted at an accelerating voltage of 20 keV and a probe current of 10 nA. Natural silicates [Jarosevich et al., 1980] and synthetic metal oxides were used as standards. Additionally, samples of Early Holocene pumice were analyzed at the IVS FEB RAS using a Vega 3 Tescan scanning electron microscope equipped with an Oxford X-max 80 $mm^2$ energy-dispersive spectrometer and AZtec software. The analysis conditions were: accelerating voltage of 20 kV, current on the nickel standard ~0.7–0.75 nA, spectrum accumulation time of 10 seconds, and electron beam diameter of 5 μm [Gorbach et al., 2022].

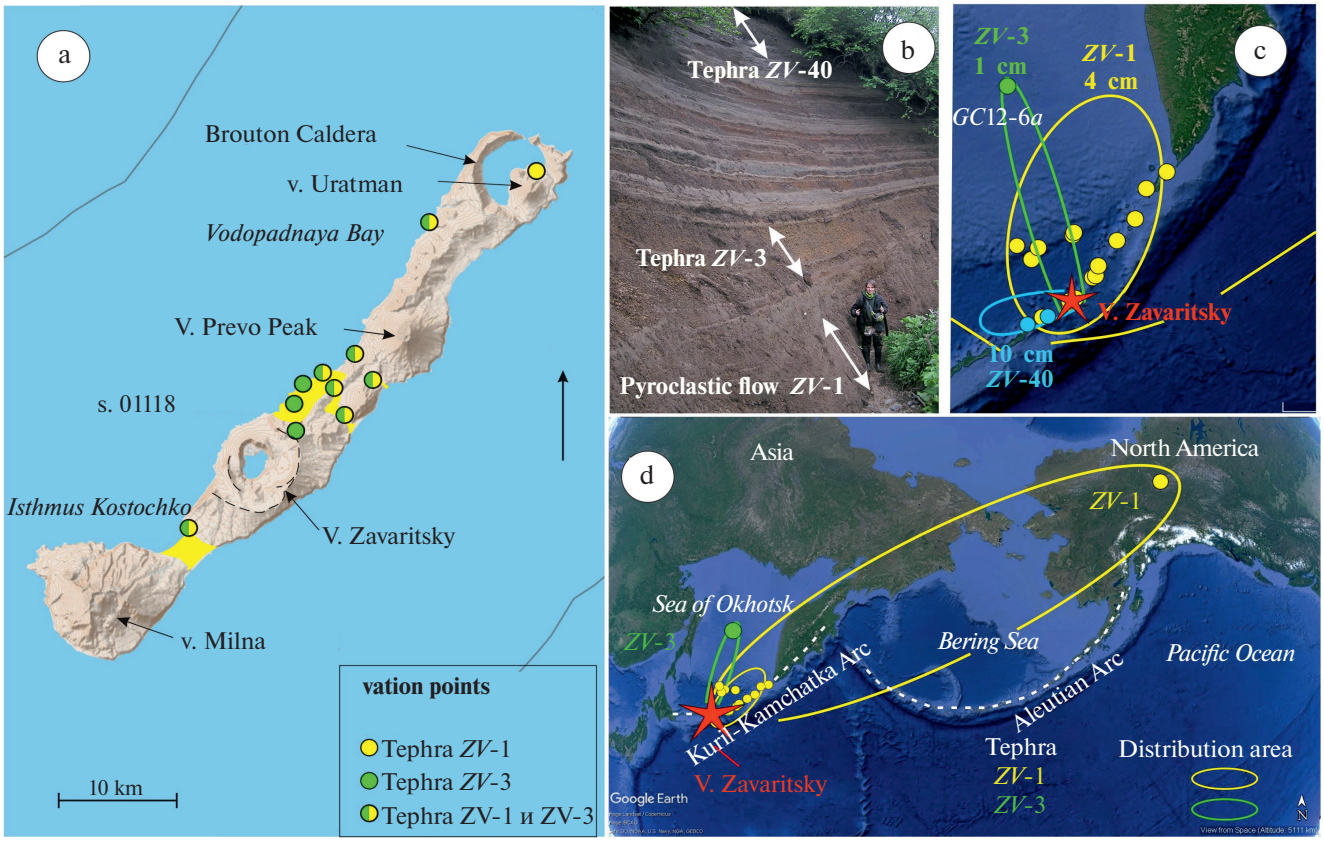


**Fig. 1.** Distribution of deposits from explosive eruptions of Zavaritsky volcano during the Holocene.
a – volcanoes of Simushir Island – circles show the location of sections where tephra ZV-1 and ZV-3 were described, yellow fill shows pyroclastic flow deposits from eruption ZV-1, dotted lines show the edges of calderas I and II, also shown is the location of reference section site 01118 (Fig. 1b); b – general view of the reference tephra section at site 01118; c – isopach maps of tephra for eruptions ZV-1 (4 cm), ZV-3 (1 cm) and ZV-40 (10 cm); d – distribution of early Holocene tephra ZV-1 (yellow line) and ZV-3 (green line); observation sites are shown in corresponding colors.

The age model for the Holocene pyroclastic section at the reference observation point (hereafter OP 01118) was created using the OxCal program [Bronk Ramsey, 2009] with the IntCal2020 calibration curve [Reimer et al., 2020] based on our radiocarbon dates for proximal deposits and published dates for Zavaritsky volcano tephras and the CKr marker tephra horizon (Table 1), taking into account the thicknesses of sandy loam layers separating the pyroclastic horizons. All ages in the text are given in calibrated years before 1950, unless otherwise specified.

## PROXIMAL PYROCLASTIC DEPOSITS OF ZAVARITSKY VOLCANO

In the most complete PPCh sections on Simushir Island, we discovered at least 40 ash horizons that formed as a result of explosive eruptions of the Zavaritsky massif over the past 10,000 years. The tephra horizons were described and studied in detail in the reference section 01118. In the lower part of the section (Fig. 1b), there are two thick layers of pumice pyroclastics formed as a

**Table 1.** Radiocarbon dates used in age model construction

| Sample number | Lab number | Sampling location | Material | Stratigraphic position | $^{14}$C age | Source |
|---|---|---|---|---|---|---|
| 01118/A1 | LE-11049 | Simushir Is. | wood | in tephra ZV-40 | 260 ± 25 | authors' data |
| 01118/A3 | LE-11050 | Simushir Is. | wood | in tephra ZV-40 | 290 ± 25 | authors' data |
| 07-US-18-10 | IAAA-72953 | Ushishir Is. | paleosol | above tephra CKr | 1910 ± 40 | Nakagawa et al., 2008 |
| 292 | AA-42209 | Chirpoi Is. | charcoal | under tephra CKr | 2178 ± 42 | Nakagawa et al., 2008 |
| 293 | AA-42209 | Chirpoi Is. | charcoal | under tephra CKr | 2290 ± 43 | Nakagawa et al., 2008 |
| 2/307 | LU-5947 | Urup Is. | peat | under tephra CKr | 2280 ± 90 | Razjigaeva et al., 2022 |
| 2/3709 | LU-6257 | Urup Is. | peat | under tephra CKr | 2140 ± 110 | Razjigaeva et al., 2022 |
| 01118/A11 | LE-11046 | Simushir Is. | paleosol | under tephra ZV-34 | 2130 ± 120 | authors' data |
| 07-SM-7-22 | IAAA-72952 | Simushir Is. | paleosol | under tephra ZV-3 | 6820 ± 40 | Nakagawa et al., 2008 |
| 08MT-1-12 | IAAA-82142 | Matua Is. | paleosol | under tephra ZV-1 | 7920 ± 50 | Nakagawa et al., 2008 |
| 08RS-2-4 | IAAA-82151 | Rashua Is. | paleosol | under tephra ZV-1 | 8100 ± 40 | Nakagawa et al., 2008 |
| B15-62 | IAAA-72598 | Paramushir Is. | peat | under tephra ZV-1 | 8540 ± 40 | Hasegawa et al., 2011 |
| – | – | Alaska | peat | calculated age of tephra ZV-1 | 9560 ± 110 | Davies, 2018 |

result of catastrophic eruptions at the beginning of the Holocene. The upper part of the section represents a fractional alternation of gray and dark gray cinder horizons deposited by smaller eruptions with interlayers of slightly humic sandy loams. The section is topped with tephra from the last powerful explosive eruption of the volcano (tephra ZV-40) (Fig. 1b).

At the base of the section lies a stratified layer of pumice pyroclastics, which we named ZV-1, consisting of a tephra horizon and overlying pyroclastic flow deposits. The thickness of tephra varies from 3–4 m on the outer slopes of the caldera to 20 cm at the northern tip of Simushir Island. The pyroclastic flow deposits are represented by slightly compacted pumice tuffs, the thickness of which is 3–5 m at a distance of 6–8 km from the caldera.

Higher up the section lies tephra from another powerful eruption (ZV-3), the thickness of which at section 01118 is about 70 cm. Unlike the ZV-1 eruption, this eruption was not accompanied by the formation of pyroclastic flows.

The numerous tephra horizons of Zavaritsky volcano lying higher up the section are well-sorted, porous, fragile cinders of gray and dark gray color. The thickness of individual horizons varies from 2 to 25 cm, and the size of fragments – from 0.5 to 10 cm (Fig. 2a). They are separated by thin (from 1 to 7 cm) interlayers of sandy loams, while rich in organic matter soil interlayers are absent, which prevented the widespread use of radiocarbon dating to determine the age of individual horizons.

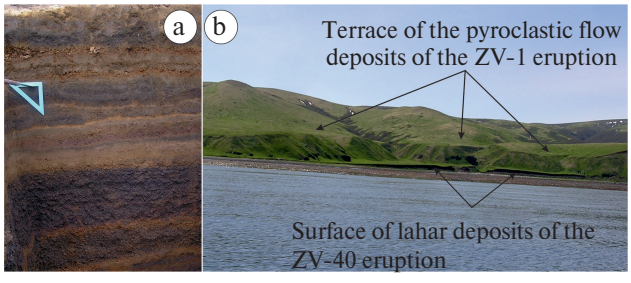


**Fig. 2.** Alternating cinder layers of Zavaritsky Volcano in a section of the pyroclastic soil cover at site 01118 (a) and lahar deposits from eruption ZV-40 on the Sea of Okhotsk shore (b).

At the very top of the section lies tephra ZV-40, formed as a result of the last major eruption of Zavaritsky volcano. The thickness of the tephra in the reference section is about 90 cm. Pyroclastic flow deposits are also absent here; however, at the top of the tephra, often with signs of erosion, lie deposits of a powerful debris flow (lahar) that spread through all the creek valleys in the periphery of the caldera complex. Upon reaching the shores of the Sea of Okhotsk and the Pacific Ocean, these deposits form gently sloping terrace-like surfaces up to 6 m high, which quickly pinch out with distance from the watercourse valley (Fig. 2b).

## VOLCANIC GLASS COMPOSITION

The composition of volcanic glass was studied in representative samples of tephra from 40 major and moderate eruptions, sampled at site 01118 (Table 2). Volcanic glasses of Holocene pyroclastics from Zavaritsky volcano correspond to low-potassium basaltic andesites–rhyolites by composition (Fig. 3a). Glasses from horizon ZV-1 show the highest SiO2 contents and correspond to rhyolites by composition (72.5–74.0 wt. % $SiO_2$); glasses from horizon ZV-3 are less silicic and correspond to dacites–rhyolites (65.0–71.9 wt. % $SiO_2$). Glasses from most eruptions have fairly homogeneous compositions (variation in $SiO_2$ – no more than 5 wt. % (Fig. 3b)). The only exception is tephra ZV-3, in which silica content in glasses varies in the range of 61.8–71.8 wt. %. Overall, wave-like changes in $SiO_2$ content are observed up the section (Fig. 4). The lowest silica contents (~55–56 wt. %) are noted around 6.4–6.3 and 2.5–1.7 thousand years BP. However, around 1650 years BP, this trend suddenly changed, and glasses of tephra from subsequent eruptions became increasingly acidic, reaching maximum values (up to 67 wt. % $SiO_2$) in tephra from the last major eruption (ZV-40). A distinctive feature of tephra from the Zavaritsky massif is the exceptionally low $K_2O$ content, which distinguishes it from tephra not only from the neighboring volcanoes Pik Prevo and Milna but also from the vast majority of other volcanoes in the Kuril Islands and Kamchatka. In the most basic glasses,

**Table 2.** Model age and mean compositions for tephra of the Holocene eruptions of Zavaritsky Volcano

| Index | Model age (BP) | | 95% probability level | | Time years (see note) | $SiO_2$ | $TiO_2$ | $Al_2O_3$ | FeO | MnO | MgO | CaO | $Na_2O$ | $K_2O$ | $P_2O_5$ | S | Cl | Total | Initial total | N |
|---|---|---|---|---|---|---|---|---|---|---|---|---|---|---|---|---|---|---|---|---|
| | mean | error | from | to | | | | | | | | | | | | | | | | |
| 1 | 2 | 3 | 4 | 5 | 6 | 7 | 8 | 9 | 10 | 11 | 12 | 13 | 14 | 15 | 16 | 17 | 18 | 19 | 20 | 21 |
| Zv#40 | 119 | 1 | 121 | 117 | 1032 | 64.02 | 0.86 | 15.53 | 7.44 | 0.23 | 1.77 | 5.79 | 3.36 | 0.66 | 0.25 | 0.00 | 0.09 | 100.00 | 98.05 | 6 |
| Zv#39 | 1151 | 184 | 1514 | 784 | 294 | 59.60 | 1.17 | 14.86 | 10.46 | 0.24 | 2.12 | 6.73 | 3.88 | 0.64 | 0.25 | 0.00 | 0.05 | 100.00 | 100.33 | 3 |
| Zv#38 | 1445 | 171 | 1773 | 1100 | 147 | 59.45 | 1.09 | 15.87 | 9.45 | 0.24 | 2.30 | 6.80 | 3.96 | 0.62 | 0.15 | 0.00 | 0.06 | 100.00 | 100.42 | 2 |
| Zv#37 | 1592 | 156 | 1884 | 1273 | 6 | 57.21 | 1.19 | 14.86 | 11.54 | 0.20 | 3.39 | 7.60 | 3.29 | 0.50 | 0.17 | 0.00 | 0.06 | 100.00 | 99.43 | 5 |
| Zv#36 | 1598 | 155 | 1886 | 1280 | 720 | 57.79 | 1.29 | 14.04 | 12.13 | 0.22 | 3.05 | 7.32 | 3.30 | 0.58 | 0.21 | 0.00 | 0.07 | 100.00 | 99.43 | 9 |
| Zv#35 | 2318 | 104 | 2535 | 2126 | 143 | 58.58 | 1.23 | 14.66 | 10.98 | 0.22 | 2.66 | 7.31 | 3.52 | 0.59 | 0.17 | 0.00 | 0.07 | 100.00 | 100.16 | 3 |
| Zv#34 | 2461 | 124 | 2716 | 2226 | 928 | 56.44 | 0.99 | 16.71 | 10.38 | 0.24 | 3.08 | 8.37 | 3.16 | 0.47 | 0.12 | 0.00 | 0.04 | 100.00 | 99.39 | 6 |
| Zv#33 | 3389 | 202 | 3802 | 2996 | 500 | 62.28 | 0.97 | 14.37 | 9.29 | 0.25 | 2.25 | 6.26 | 3.45 | 0.67 | 0.14 | 0.00 | 0.06 | 100.00 | 98.74 | 3 |
| Zv#32 | 3889 | 226 | 4354 | 3446 | 285 | 60.81 | 1.16 | 14.04 | 11.53 | 0.23 | 2.49 | 6.91 | 1.68 | 0.78 | 0.23 | 0.01 | 0.14 | 100.00 | 94.73 | 3 |
| Zv#31 | 4174 | 237 | 4653 | 3706 | 286 | 61.16 | 0.91 | 15.30 | 9.08 | 0.20 | 1.90 | 6.44 | 4.06 | 0.68 | 0.19 | 0.00 | 0.07 | 100.00 | 99.21 | 6 |
| Zv#30 | 4460 | 246 | 4956 | 3972 | 285 | 59.74 | 1.01 | 15.88 | 9.52 | 0.17 | 1.78 | 7.00 | 3.92 | 0.69 | 0.23 | 0.00 | 0.06 | 100.00 | 100.48 | 6 |
| Zv#29 | 4745 | 253 | 5259 | 4246 | 72 | 60.43 | 0.99 | 15.11 | 9.72 | 0.22 | 2.28 | 6.76 | 3.59 | 0.64 | 0.20 | 0.00 | 0.07 | 100.00 | 100.41 | 3 |
| Zv#28 | 4817 | 255 | 5331 | 4312 | 214 | 62.14 | 1.02 | 14.94 | 9.69 | 0.20 | 2.27 | 6.63 | 1.99 | 0.72 | 0.24 | 0.04 | 0.09 | 100.00 | 96.07 | 5 |
| Zv#27 | 5031 | 259 | 5549 | 4519 | 2 | 61.44 | 0.94 | 16.24 | 7.90 | 0.16 | 1.55 | 6.71 | 4.05 | 0.74 | 0.19 | 0.00 | 0.08 | 100.00 | 99.70 | 3 |
| Zv#26 | 5033 | 259 | 5561 | 4527 | 141 | 60.37 | 1.00 | 14.80 | 10.13 | 0.20 | 2.65 | 6.79 | 3.26 | 0.58 | 0.13 | 0.00 | 0.09 | 100.00 | 99.07 | 5 |
| Zv#25 | 5174 | 259 | 5693 | 4659 | 141 | 60.65 | 0.90 | 15.82 | 9.14 | 0.20 | 2.04 | 6.88 | 3.55 | 0.54 | 0.19 | 0.00 | 0.09 | 100.00 | 98.99 | 3 |
| Zv#24 | 5315 | 259 | 5840 | 4804 | 423 | 59.28 | 0.92 | 15.88 | 9.55 | 0.21 | 2.47 | 7.33 | 3.60 | 0.54 | 0.17 | 0.00 | 0.04 | 100.00 | 99.48 | 3 |
| Zv#23 | 5738 | 261 | 6260 | 5215 | 352 | 59.25 | 0.78 | 16.72 | 8.83 | 0.23 | 2.59 | 7.36 | 3.83 | 0.41 | 0.00 | 0.00 | 0.00 | 100.00 | 101.15 | 2 |
| Zv#22 | 6090 | 265 | 6618 | 5562 | 70 | 56.46 | 1.07 | 15.57 | 12.21 | 0.23 | 3.49 | 8.31 | 1.88 | 0.53 | 0.17 | 0.01 | 0.06 | 100.00 | 97.08 | 3 |
| Zv#21 | 6160 | 266 | 6690 | 5633 | 141 | 57.21 | 1.33 | 14.07 | 13.16 | 0.24 | 2.84 | 7.71 | 2.63 | 0.58 | 0.18 | 0.00 | 0.05 | 100.00 | 99.62 | 4 |
| Zv#20 | 6301 | 268 | 6836 | 5775 | 71 | 55.40 | 1.06 | 15.91 | 11.64 | 0.24 | 3.90 | 8.71 | 2.61 | 0.39 | 0.10 | 0.00 | 0.06 | 100.00 | 100.77 | 3 |

**Table 2.** *Continued*

| Index | Model age (BP) | | 95% probability level | | Time years (see note) | $SiO_2$ | $TiO_2$ | $Al_2O_3$ | FeO | MnO | MgO | CaO | $Na_2O$ | $K_2O$ | $P_2O_5$ | S | Cl | Total | Initial total | N |
|---|---|---|---|---|---|---|---|---|---|---|---|---|---|---|---|---|---|---|---|---|
| | mean | error | from | to | | | | | | | | | | | | | | | | |
| 1 | 2 | 3 | 4 | 5 | 6 | 7 | 8 | 9 | 10 | 11 | 12 | 13 | 14 | 15 | 16 | 17 | 18 | 19 | 20 | 21 |
| Zv#19 | 6372 | 269 | 6906 | 5845 | 211 | 57.35 | 1.23 | 14.38 | 12.37 | 0.26 | 3.35 | 7.79 | 2.54 | 0.53 | 0.12 | 0.00 | 0.07 | 100.00 | 99.56 | 3 |
| Zv#18 | 6583 | 274 | 7121 | 6065 | 423 | 60.99 | 0.96 | 15.01 | 9.36 | 0.20 | 2.17 | 6.58 | 3.81 | 0.64 | 0.21 | 0.00 | 0.07 | 100.00 | 99.94 | 3 |
| Zv#17 | 7006 | 284 | 7535 | 6504 | 71 | 63.40 | 0.90 | 14.73 | 9.31 | 0.22 | 2.05 | 6.02 | 2.27 | 0.69 | 0.19 | 0.11 | 0.10 | 100.00 | 96.86 | 4 |
| Zv#16 | 7077 | 286 | 7598 | 6573 | 141 | 62.34 | 0.90 | 15.08 | 8.66 | 0.20 | 2.05 | 6.11 | 3.81 | 0.67 | 0.10 | 0.00 | 0.08 | 100.00 | 98.50 | 3 |
| Zv#15 | 7218 | 290 | 7733 | 6725 | 70 | 61.43 | 0.87 | 15.36 | 8.76 | 0.21 | 2.16 | 6.36 | 3.96 | 0.59 | 0.21 | 0.00 | 0.08 | 100.00 | 99.43 | 3 |
| Zv#14 | 7288 | 293 | 7800 | 6796 | 2 | 62.77 | 0.86 | 15.16 | 8.15 | 0.20 | 2.01 | 5.97 | 3.99 | 0.62 | 0.19 | 0.00 | 0.08 | 100.00 | 99.49 | 3 |
| Zv#13 | 7290 | 293 | 7800 | 6798 | 282 | 63.48 | 0.91 | 14.39 | 8.74 | 0.23 | 1.93 | 5.69 | 3.66 | 0.68 | 0.19 | 0.00 | 0.10 | 100.00 | 98.99 | 6 |
| Zv#12 | 7572 | 290 | 8063 | 7100 | 141 | 67.57 | 0.83 | 14.81 | 7.03 | 0.16 | 1.01 | 4.97 | 2.43 | 0.83 | 0.23 | 0.01 | 0.13 | 100.00 | 96.91 | 4 |
| Zv#11 | 7713 | 288 | 8195 | 7255 | 71 | 64.47 | 0.75 | 14.44 | 7.64 | 0.21 | 2.21 | 5.22 | 4.15 | 0.64 | 0.18 | 0.00 | 0.09 | 100.00 | 100.99 | 3 |
| Zv#10 | 7784 | 287 | 8261 | 7333 | 141 | 65.96 | 0.83 | 14.29 | 8.07 | 0.19 | 1.91 | 5.46 | 2.05 | 0.84 | 0.26 | 0.02 | 0.12 | 100.00 | 96.65 | 3 |
| Zv#9 | 7925 | 285 | 8391 | 7485 | 212 | 64.96 | 0.73 | 14.70 | 7.33 | 0.19 | 1.78 | 5.31 | 3.89 | 0.73 | 0.27 | 0.00 | 0.11 | 100.00 | 99.61 | 3 |
| Zv#8 | 8137 | 282 | 8570 | 7715 | 3 | 65.32 | 0.63 | 15.26 | 6.42 | 0.20 | 1.41 | 5.33 | 4.36 | 0.77 | 0.20 | 0.00 | 0.09 | 100.00 | 99.68 | 6 |
| Zv#7 | 8140 | 282 | 8575 | 7717 | 505 | 63.10 | 0.91 | 14.74 | 8.64 | 0.19 | 2.21 | 6.02 | 3.19 | 0.72 | 0.19 | 0.00 | 0.10 | 100.00 | 97.87 | 3 |
| Zv#6 | 8645 | 232 | 9003 | 8288 | 72 | 65.96 | 0.67 | 14.74 | 6.70 | 0.16 | 1.27 | 5.08 | 4.28 | 0.79 | 0.22 | 0.00 | 0.11 | 100.00 | 99.45 | 3 |
| Zv#5 | 8717 | 224 | 9060 | 8370 | 72 | 64.65 | 0.82 | 14.45 | 8.86 | 0.21 | 2.06 | 5.74 | 1.96 | 0.79 | 0.25 | 0.05 | 0.18 | 100.00 | 96.25 | 4 |
| Zv#4 | 8789 | 216 | 9120 | 8456 | 217 | 64.12 | 0.70 | 15.13 | 7.50 | 0.16 | 1.64 | 5.86 | 3.96 | 0.72 | 0.10 | 0.00 | 0.11 | 100.00 | 99.11 | 6 |
| Zv#3 | 9 | 190 | 9285 | 8716 | 226 | 67.23 | 0.62 | 14.23 | 6.43 | 0.03 | 1.37 | 4.93 | 4.20 | 0.84 | 0.05 | 0.00 | 0.08 | 100.00 | 99.71 | 87 |
| Zv#2 | 9232 | 138 | 9440 | 9001 | 233 | 65.51 | 0.65 | 14.63 | 7.39 | 0.21 | 1.70 | 5.16 | 3.65 | 0.75 | 0.22 | 0.00 | 0.11 | 100.00 | 99.92 | 3 |
| Zv#1 | 9465 | 64 | 9546 | 9333 | 0 | 73.49 | 0.48 | 12.95 | 3.98 | 0.01 | 0.55 | 2.87 | 4.47 | 1.01 | 0.03 | 0.00 | 0.16 | 100.00 | 98.08 | 106 |

Note: Time means the time interval between two adjacent eruptions; contents of rock-forming oxides and volatile components are in wt. %; N is the number of analyses for a given tephra.

$K_2O$ content is 0.3–0.5 wt. %, and in the most silicic glasses, it does not exceed 0.9–1.0 wt. %.

## AGE AND MAGNITUDE OF CATASTROPHIC ERUPTIONS OF ZAVARITSKY VOLCANO AND DISTRIBUTION OF THEIR TEPHRA

The stratigraphic position of the ZV-1 and ZV-3 pumice horizons and their specific geochemical characteristics allowed us to confidently identify these horizons in the sections of Simushir Island, as well as to correlate them with the distal ash layers described by us and other authors in the sections of the Kuril Islands [Nakagawa et al., 2008; Hasegawa et al., 2011], in marine cores from the Sea of Okhotsk [Derkachev et al., 2016], and in a peat bog in northwestern Canada [Davies, 2018].

Tephra ZV-1. Regional tephrochronological studies in the Kuril Islands revealed the presence of low-potassium rhyolitic ash in the lower part of many sections of Holocene deposits in the Central and Northern Kurils (Fig. 1c). The tephra, given the index ZvSu and associated, according to the authors, with one of the eruptions of Zavaritsky volcano, is described on the islands of Rasshua (where its thickness is 10–15 cm), Matua (5 cm), Shiashkotan (4–5 cm), and Onekotan (4 cm) [Nakagawa et al., 2008]. At the same time, south of Simushir, on the islands of Chirpoi and Urup, this tephra is absent. Tephrochronological studies on Paramushir Island revealed a unique ash for this island (index GA) with a very low content of $K_2O$, which was 3–4 cm thick [Hasegawa et al., 2011]. In the soil-pyroclastic cover sections, this tephra lies below the KO tephra horizon associated with the caldera-forming eruption of Kurilskoye Lake in Southern Kamchatka [Hasegawa et al., 2011]. An ash with similar geochemical characteristics labeled TR(ZV) was found in sediment cores in the Sea of Okhotsk (Derkachev et al., 2016). In addition to the glass composition corresponding to low-potassium rhyolites, the identification features of these tephras also include peculiarities of the mineralogical composition: the presence of clino- and orthopyroxene with the absence of amphibole [Hasegawa et al., 2011]. One more Early Holocene low-potassium rhyolitic cryptotephra, similar in its geochemical characteristics to the pyroclastics of the Zavaritsky caldera was found in a peat bog in northwestern Canada [Davies, 2018].

Analysis of the published data on the composition of tephras ZvSu, GA and TR(Zv), as well as cryptotephra from the northwest of Canada, presented in these works, showed that both stratigraphically and by glass compositions they are identical to the proximal pumice ZV-1 (Fig. 3b), this means that they are products of the same eruption. The discovery of ZV-1 tephra in sections of the Northern and Central Kuriles, as well as in cores from the Sea of Okhotsk and in the northwest of Canada, and its absence in sections south of Simushir Island indicates that tephra dispersed predominantly in the northeastern direction. The northeast direction of the ash fall axis and the discovery of this tephra in northwestern Canada obviously implies its deposition in the territories of Kamchatka, Chukotka, and Alaska; the area of ash fall was more than 6 million $km^2$ (Fig. 1d).

Available data [Nakagawa et al., 2008; Hasegawa et al., 2011; Derkachev et al., 2016] allowed us to delineate the ashfall zone with a thickness of 4 cm and estimate its area at 250 thousand $km^2$ (Fig. 1c). According to minimum estimates (following [Legros, 2002]), the volume of erupted tephra is 36.9 $km^3$, and the total volume of pyroclastics from the ZV-1 eruption, taking into account pyroclastic flow deposits on land, can be estimated at 37.0 $km^3$ (or ~15 $km^3$ converted to dense rock equivalent). This estimate is conservative and does not account for the volume of pyroclastic flow deposits on the ocean floor, and may also underestimate the volume of distal tephra. The minimum estimate of the eruption magnitude ($M$), with a bulk pumice density of 700 $kg/m^3$, is 6.4. Unfortunately, methods for estimating ash volume that account for cryptotephra have not yet been developed, but the very fact that ZV-1 tephra particles were found in northwestern Canada at a distance of almost 4500 km from the volcano indicates an exceptionally powerful eruption (Fig. 1d).

Thus, even the minimum estimate of the erupted pyroclastic volume places the ZV-1 eruption among the largest in the Kuril-Kamchatka arc during the last 10 thousand years. In terms of volume, it is second only to the eruption that produced the Kurile Lake caldera, but exceeds all known eruptions of the Kuril Islands volcanoes during the Holocene. Such large volumes of erupted pyroclastic material indicate that the ZV-1 eruption may be associated with the formation of the last caldera in the Zavaritsky massif (caldera II, according to [Gorshkov, 1967]), although this statement needs additional confirmation. Estimates of the tephra age range from 8.9 [Nakagawa et al., 2008] to 9.6 [Davies, 2018] thousand years; in our model, the age of this eruption is 9,462 ± 67 years. These age estimates are consistent with the position of ZV-1 tephra below the KO tephra dated to about 8.4 thousand years [Ponomareva et al., 2004].

Tephra ZV-3. This tephra, which according to our model is about 9.2 thousand years old, was found in sections north of the Zavaritsky caldera, up to Vodopadnaya Bay, but it is absent in Broughton Bay on the northeast of the island (Fig. 1a). To the southwest of the caldera, it is described on its outer slope and on the Kostochko isthmus (Fig. 1a), but is absent on Urup Island. This indicates that the axis of ash fall was directed to the NNW and the vast majority of tephra fell into the Sea of Okhotsk, which makes it difficult to calculate its volume. To assess the area of tephra distribution, data from studies of sedimentary cores in the Sea of Okhotsk were analyzed. In core GC12-6A (Fig. 1c), a low-potassium tephra (index N) [Derkachev et al., 2016] with a thickness of 1 cm was found, which by glass composition is identical to the ZV-3 ash (Fig. 3c). The authors associated it with the eruption of the Gamchen volcano in Kamchatka, however, comparison of the compositions of N tephra glass and Gamchen volcano pyroclastics does not support this conclusion (Fig. 3c). Additionally, there are no known explosive eruptions for the Gamchen volcano in the early Holocene: its cone began to form only ~3.6 thousand years ago [Kozhurin et al., 2006]. In our opinion, tephra N is a distal analog of tephra ZV-3, indicating its distribution in the northern direction for a distance of more than 700 km (Fig. 1d). The minimum volume of tephra ZV-3 (according to [Legros, 2000]) can be estimated at 5.5 $km^3$, and the minimum magnitude of the eruption at 5.6.

Tephra ZV-40. This tephra, indexed as ZAV-1, was described in several publications on the Middle Kuriles. Radiocarbon dates of this tephra found in literature range from 1070 ± 70 to 40 ± 90 $^{14}C$ years [Razzhigaeva et al., 2013; Nakagawa et al., 2008; Razjigaeva et al., 2022], averaging about 600 $^{14}C$ years. However, most of these dates were obtained from the soil underlying the tephra, i.e., they characterized exclusively the time range of this soil formation and could provide an older age estimate for the tephra covering it. The date 40 ± 90 $^{14}C$ years was obtained from a section with a distinct age inversion [Razzhigaeva et al., 2013] and was not considered when calculating the age. To obtain a more accurate age, we dated charred plant remains (branches and stems of shrubs) found directly in the ZAV-1 tephra. The obtained dates of 260 ± 25 and 290 ± 25 (see Table 1) indicate a younger age of the tephra. Calibration of these dates shows that the eruption occurred about 150–430 years ago. An even more precise age of this eruption was determined as a result of studying ice cores from Greenland [Hutchison, personal communication]. In four boreholes (NEEM-2011-S1, NGRIP1, B19, and Tunu2013) in the ice horizon formed, according to preliminary data, shortly before the mid-19th century, a zone of increased concentration of ash particles was found. The geochemical analysis of volcanic glass from this horizon showed that the composition of the ash particle glasses is identical to the composition of ZV-40 tephra glasses [Hutchison, personal communication]. Thus, it can be confidently stated that the ZV-40 eruption occurred around 1830–1850 CE. In the soil-pyroclastic cover sections, the ZV-40 tephra was found on the islands of Simushir, Chirpoi, and Urup. Spatial variations in the thickness of the tephra horizon suggest that the ash fall axis was directed southwest (Fig. 1c): in the northeast direction, the tephra wedges

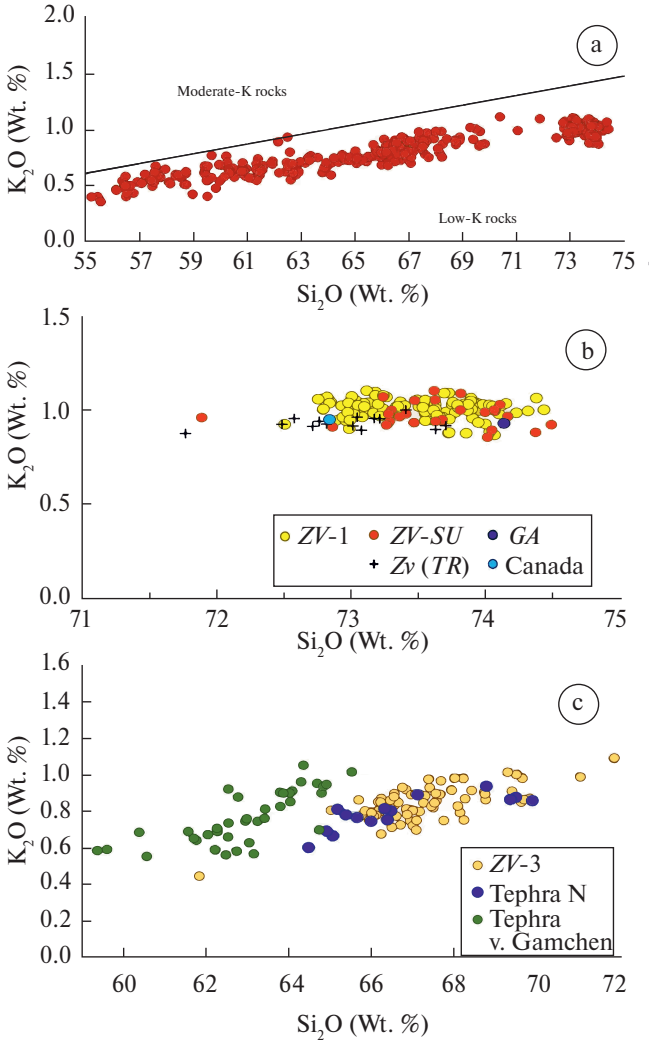


**Fig. 3.** The $SiO_2$-$K_2O$ diagrams for volcanic glasses in the Holocene pyroclastics discharged by Zavaritsky Volcano.
a – classification diagram $K_2O$–$SiO_2$ for all studied glasses. The boundary between medium- and low-potassium compositions is shown after [Le Maitre et al., 2002]; b – glass compositions in proximal and distal samples of tephra ZV-1 (see text for explanation); c – glass compositions in proximal and distal samples of tephra ZV-3, also shown are glass compositions from Gamchen volcano according to [Portnyagin et al., 2020].

out very quickly, and in the north of Simushir Island (at a distance of 30 km from the caldera), its thickness is only 1–2 cm, while on the islands of Chirpoi and Urup, i.e., at a distance of 100–130 km from the eruption center, the thickness of the ZV-40 tephra reaches 10–12 cm. The limited number of observation points allowed us to determine only the minimum volume of ejected material. Calculated using the method of [Legros, 2000], it amounted to about 3.5 $km^3$. The magnitude of the eruption was at least 5.4.

## EXPLOSIVE ACTIVITY IN THE MIDDLE-LATE HOLOCENE AND CHANGES IN VOLCANIC GLASS COMPOSITION IN TEPHRAS

Eruptions that followed the emissions of the pumice tephras ZV-1 and ZV-3 were of a more modest scale, and their tephras have been discovered only within Simushir Island. During the period 9.8–7.3 thousand years ago, glasses in the tephra mainly correspond to dacites (Fig. 4). Then the $SiO_2$ content in glasses gradually decreases and reaches a minimum (55 wt%) around 6.4 thousand years ago. After this, for approximately 2.3 thousand years, there are tephra eruptions with glasses of andesitic composition, but around 2.5–1.6 thousand years ago, the $SiO_2$ content drops again to the values of low-$SiO_2$ andesites – andesite-basalts. Glasses of tephras from subsequent moderate eruptions demonstrate some increase in $SiO_2$ content; however, after a significant break, the third strong explosive eruption in the Holocene (ZV-40) follows, in which the $SiO_2$ content in glasses increases sharply. In the tephra of this eruption, glasses with an elevated silica content (up to 67.6 wt%) reappear, similar to the glasses of early Holocene eruptions (Fig. 4).

Undulating fluctuations in $SiO_2$ content in glasses from pyroclastics of major eruptions were previously noted for the Kamchatka volcanoes Shiveluch [Ponomareva et al., 2015] and Klyuchevskoy [Portnyagin et al., 2009]. Since volcanic glasses represent fragments of partially degassed melt, quenched when ejected into the atmosphere, their compositions reflect the evolution of magma in the chamber. Tephras with the most silicic glasses correspond to the removal of maximally differentiated material that has evolved in the chamber for a long time without significant influx of fresh magma; pyroclastics with the most basic glasses indicate the entry

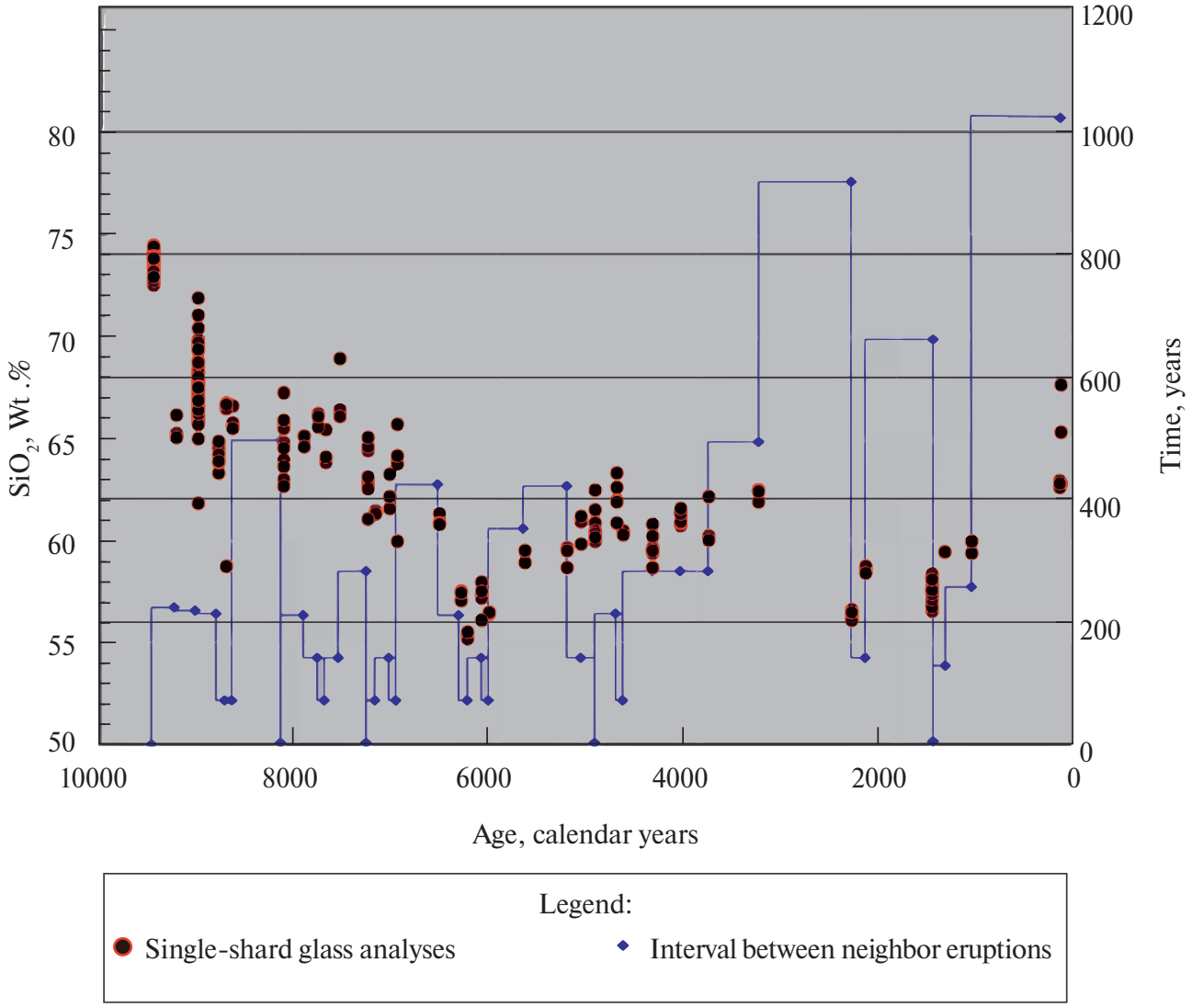


**Fig. 4.** Changes in $SiO_2$ content in volcanic glasses of Zavaritsky volcano tephra and intervals between eruptions over the past 10,000 years.

into the chamber and rapid removal to the surface of fresh, least differentiated magmas. Accordingly, the downward trend in $SiO_2$ content characterizes the gradual replacement of differentiated magma with fresh portions, while the upward trend indicates a slowdown in the supply of fresh magma and the gradual predominance of differentiated varieties in the chamber. The increase in $SiO_2$ content after 1.5 thousand years ago (Fig. 4) may indicate the preparation for a new powerful eruption.

In general, the regime of the volcano's activity over the past 10 thousand years is quite unusual (Fig. 4). In the early and middle Holocene (until 4000 years ago), large and moderate explosive eruptions occurred fairly regularly, with intervals between eruptions averaging about 200 years. However, after 4000 years ago, the activity regime changed significantly. Between explosive eruptions, there began to be long (up to 900 years) intervals, followed by one or several eruptions with a gap of 100–250 years. The last long period of "quiescence" ended with the ZV-40 eruption and, if the proposed pattern is correct, a rather strong explosive eruption should be expected on Zavaritsky volcano in the next 100 years.

## CONCLUSIONS

1. Zavaritsky volcano in the Holocene was one of the most active volcanoes of the Kuril island arc.

2. Volcanic glasses of Holocene pyroclastics of Zavaritsky volcano correspond in composition to low-potassium basaltic andesites-rhyolites and show undulating variations from 55 to 75 wt. % $SiO_2$. The most silicic (rhyolitic) glasses are noted in the pumices of the very first Holocene eruption ZV-1.

3. The strongest eruption was the ZV-1 eruption, which occurred about 9.5 thousand years ago. The eruption had a magnitude of 6.4. The tephra from this eruption spread at least 4500 km to the NE. The volume of tephra was about 37 $km^3$. Due to its wide distribution and compositional characteristics, the ZV-1 tephra can serve as an excellent marker for correlation and synchronization of marine and terrestrial paleoarchives over a vast area from the Sea of Okhotsk to the NW part of North America.

4. The tephra of the subsequent eruption ZV-3 spread to a distance of at least 700 km. The volume of tephra was about 5.5 $km^3$.

5. The increase in $SiO_2$ content in the glass of the last major eruption ZV-40 (which occurred around 1830-1850) to early Holocene values, coinciding with an increase in eruption magnitude, as well as a long period of quiescence before this eruption may indicate the preparation for a new powerful explosive eruption in the next 100 years.

## CONFLICT OF INTEREST

The authors of this work declare that they have no conflict of interest.

## FUNDING

The study was carried out with the support of the Russian Science Foundation Grant No. 22-17-00074, https://rscf.ru/project/22-17-00074/ .

## REFERENCES

1. *Gorbach N.V., Filosofova T.M., Melnikov D.V., Manevich T.M.* Composition of volcanic glasses in products of summit eruption and G.S. Gorshkov flank vent at Klyuchevskoy volcano in 2020–2021: comparative analysis and interpretation // Journal of Volcanology and Seismology. 2022. No. 2. Pp. 28-37.
2. *Gorshkov G.S.* Volcanism of the Kuril Island Arc. Moscow: Nauka, 1967. 288 p.
3. *Degterev A.V., Rybin A.V., Melekestsev I.V., Razzhigaeva N.G.* Explosive eruptions of Sarychev Peak volcano in the Holocene (Matua Island, Central Kuriles): tephra geochemistry // Pacific Geology. 2012. Vol. 31. No. 6. Pp. 16–26.
4. *Melekestsev I.V., Egorova I.A., Lupikina E.G.* Internal ridge of the Kuril arc // Kamchatka, Kuril and Commander Islands. Moscow: Nauka, 1974. Pp. 265–327.
5. *Parfenova O.V., Burikova I.A., Dril S.I.* Evolution features of silicic rocks composition of low-potassium calc-alkaline series of Zavaritsky volcano (Kuril island arc, Simushir Island) // Moscow University Bulletin. Series 4. Geology. 2015. No. 6. Pp. 53–61.
6. *Razzhigaeva N.G., Ganzey L.A., Belyanina N.I., Grebennikova T.A., Arslanov Kh.A., Pshenichnikova N.F., Rybin A.V.* The role of climatic and volcanic factors in the formation of organogenic deposits and landscape development of Simushir Island (Central Kuriles) in the Middle-Late Holocene // Pacific Geology. 2013. Vol. 32. No. 3. Pp. 55–67.
7. *Baldini J.U., Brown R.J., McElwaine J.N.* Was millennial scale climate change during the Last Glacial triggered by explosive volcanism? // Scientific Reports. 2015. Vol. 5(1). Pp. 1–9.
8. *Bronk Ramsey C.* Bayesian Analysis of Radiocarbon Dates // Radiocarbon. 2009. Vol. 51. Pp. 337–360.
9. *Davies L.J.* The Development of a Holocene Cryptotephra Framework in Northwestern North America / PhD thesis. Edmonton: University of Alberta, 2018. 235 p.
10. *Derkachev A.N., Nikolaeva N.A., Gorbarenko S.A., Portnyagin M.V., Ponomareva V.V., Nürnberg D., Sakamoto T., Iijima K., Liu Y., Shi X., Lu H., Wang K.* Tephra layers in the Quaternary deposits of the Sea of Okhotsk: Distribution, composition, age and

volcanic sources // Quaternary International. 2016. Vol. 425. Pp. 248–272.

**11.** *Hasegawa T., Nakagawa M., Yoshimoto M., Ishizuka Y., Hirose W. Seki S., Ponomareva V., Rybin A.* Tephrostratigraphy and petrological study of Chikurachki and Fuss volcanoes, western Paramushir Island, northern Kurile Islands: Evaluation of Holocene eruptive activity and temporal change of magma system // Quaternary International. 2011. Vol. 246. Pp. 278–297.

**12.** *Jarosewich E., Nelen J.A., Norberg J.A.* Reference samples for electron microprobe analysis // Geostandart Newsletters. 1980. Vol. 4(1). Pp. 43–47.

**13.** *Kozhurin A., Acocella V., Kyle P.R., Lagmay F.M., Melekestsev I.V., Ponomareva V., Rust D., Tibaldi A., Tunesi A., Corazzato C., Rovida A., Sakharov A., Tengonciang A., Uy H.* Trenching studies of active faults in Kamchatka, eastern Russia: paleoseismic, tectonic and hazard implications // Tectonophysics. 2006. Vol. 417. Pp. 285–304.

**14.** *Legros F.* Minimum volume of a tephra fallout deposit estimated from a single isopach // Journal of Volcanology and Geothermal Research. 2000. Vol. 96. Pp. 25–32.

**15.** *Le Maitre R.W., Streckeisen A., Zanettin B., Le Bas M.J., Bonin B., Bateman P., Bellieni G., Dudek A., Efremova S., Keller J., Lameyre J.A., Sabine P.A., Schmid R., Sorensen H. Wooley A.R.* Igneous Rocks: A Classification and Glossary of Terms: A Classification and Glossary of Terms: Recommendations of the International Union of Geological Sciences, Subcommission on the Systematics of Igneous Rocks. Cambridge: Cambridge University Press, 2002.

**16.** *McConnell J.R., Sigl M., Plunkett G., Burke A., Kim W.M., Raible C.C., Wilson A.I., Manning J.G., Ludlow F., Chellman N.J., Innes H.M.* Extreme climate after massive eruption of Alaska's Okmok volcano in 43 BCE and effects on the late Roman Republic and Ptolemaic Kingdom // Proceedings of the National Academy of Sciences. 2020. Vol. 117. No. 27. Pp. 15443–15449.

**17.** *Nakagawa M., Ishizuka Y., Kudo T., Yoshimoto M., Hirose W., Ishizaki Y., Gouchi N., Katsui Y., Solovyov A., Steinberg G., Abdurakhmanov A.* Tyatya Volcano, southwestern Kuril Arc: Recent eruptive activity inferred from widespread tephra // Island Arc. 2002. Vol. 11. Pp. 236–254.

**18.** *Nakagawa M., Ishizuka Y., Hasegawa T., Baba A., Kosugi A.* Preliminary Report on Volcanological Research of KBP 2007-08 Cruise by Japanese Volcanology group. Sapporo, Japan: Hokkaido University, 2008. Unpublished report (tDAR ID: 391304)

**19.** *Ponomareva V.V., Kyle P.R., Melekestsev I.V., Rinkleff P.G., Dirksen O.V., Sulerzhitsky L.D., Zaretskaia N.E., Rourke R.* The 7600 ($^{14}$C) year BP Kurile Lake caldera-forming eruption, Kamchatka, Russia: stratigraphy and field relationships // Journal of Volcanology and Geothermal Research. 2004. Vol. 136. Pp. 199-222.

**20.** *Ponomareva V., Portnyagin M., Pevzner M., Blaauw M., Kyle Ph., Derkachev A.* Tephra from andesitic Shiveluch volcano, Kamchatka, NW Pacific: Chronology of explosive eruptions and geochemical fingerprinting of volcanic glass // International Journal of Earth Sciences (Geol Rundschau). 2015. Vol. 104. Pp. 1459–1482.

**21.** *Portnyagin M., Ponomareva V., Bindeman I., Hauff F., Krasheninnikov S., Kuvikas O., Mironov N., Pletchova A., van den Bogaard C., Hoernle K.* Millennial variations of major and trace element and isotope compositions of Klyuchevskoy magmas, Kamchatka // Terra Nostra. 2009. Vol. 1. Pp. 64–65.

**22.** *Portnyagin M.V., Ponomareva V.V., Zelenin E.A., Bazanova L.I., Pevzner M.M., Plechova A.A., Rogozin A.N., Garbe-Schönberg D.* TephraKam: geochemical database of glass compositions in tephra and welded tuffs from the Kamchatka volcanic arc (northwestern Pacific) // Earth System Science Data. 2020. Vol. 12(1). P. 469–486.

**23.** *Razjigaeva N.G., Ganzey L.A., Arslanov K.A., Pshenichnikova N.F.* Coastal dunes of Urup Island (Kuril Islands, North-Western Pacific): Palaeoclimatic and environmental archive // Geosystems of Transition Zones. 2022. Vol. 6. Pp. 100–113.

**24.** *Reimer P., Austin W., Bard E., Bayliss A., Blackwell P., Bronk Ramsey C., Butzin M., Cheng H., Edwards R., Friedrich M., Grootes P., Guilderson T., Hajdas I., Heaton T., Hogg A., Hughen K., Kromer B., Manning S., Muscheler R., Palmer J., Pearson C., van der Plicht J., Reimer R., Richards D., Scott E.,*

*Southon J., Turney C., Wacker L., Adolphi F., Büntgen U., Capano M., Fahrni S., Fogtmann-Schulz A., Friedrich R., Köhler P., Kudsk S., Miyake F., Olsen J., Reinig F., Sakamoto M., Sookdeo A., Talamo S.* The IntCal20 Northern Hemisphere radiocarbon age calibration curve (0-55 cal kBP) // Radiocarbon. 2020. Vol. 62. Pp. 725–757.